JOURNAL OF VIROLOGY, Sept. 1996, p. 6251–6259 Vol. 70, No. 9
0022-538X/96/$04.00+0

Apoptotic Suppression by Baculovirus P35 Involves Cleavage by and Inhibition of a Virus-Induced CED-3/ICE-Like Protease

JOHN BERTIN,[1]† SUSAN M. MENDRYSA,[1] DOUGLAS J. LACOUNT,[1] SMITA GAUR,[2] JOSEPH F. KREBS,[2] ROBERT C. ARMSTRONG,[2] KEVIN J. TOMASELLI,[2] AND PAUL D. FRIESEN[1]*

Institute for Molecular Virology and Department of Biochemistry, University of Wisconsin—Madison, Madison, Wisconsin 53706,[1] and IDUN Pharmaceuticals, Inc., La Jolla, California 92037[2]

Received 14 May 1996/Accepted 12 June 1996

Baculovirus *p35* prevents programmed cell death in diverse organisms and encodes a protein inhibitor (P35) of the CED-3/interleukin-1β-converting enzyme (ICE)-related proteases. By using site-directed mutagenesis, we have identified P35 domains necessary for suppression of virus-induced apoptosis in insect cells, the context in which P35 evolved. During infection, P35 was cleaved within an essential domain at or near the site DQMD-87G required for cleavage by CED-3/ICE family proteases. Cleavage site substitution of alanine for aspartic acid at position 87 (D87A) of the P_1 residue abolished P35 cleavage and antiapoptotic activity. Although the P_4 residue substitution D84A also caused loss of apoptotic suppression, it did not eliminate cleavage and suggested that P35 cleavage is not sufficient for antiapoptotic activity. Apoptotic insect cells contained a CED-3/ICE-like activity that cleaved in vitro-translated P35 and was inhibited by recombinant wild-type P35 but not P_1- or P_4-mutated P35. Thus, baculovirus infection directly or indirectly activates a novel CED-3/ICE-like protease that is inhibited by P35, thereby preventing virus-induced apoptosis. Our findings confirmed the inhibitory activity of P35 towards the CED-3/ICE proteases, including recombinant mammalian enzymes, and were consistent with a mechanism involving P35 stoichiometric interaction and cleavage. P35's inhibition of phylogenetically diverse proteases accounts for its general effectiveness as an apoptotic suppressor.

Programmed cell death, or apoptosis, is an active process of cellular self-destruction that is involved in normal development, tissue homeostasis, and the pathogenesis of various diseases, including those caused by viral infection. Molecular components of the cell death program are highly conserved among vertebrates and invertebrates (reviewed in references 36, 40, 43, 45). As indicated by the requirement for the interleukin-1β-converting enzyme (ICE)-related gene *ced-3* in programmed cell death of *Caenorhabditis elegans* and the identification of *ced-3*/*ice* homologs in vertebrates (10, 11, 39, 44, 47), the apoptotic program includes participation of one or more members of the CED-3/ICE family of cysteine proteases. Current evidence suggests that diverse signals converge to activate the death proteases, thereby implying that these enzymes play a key role in the apoptotic program (reviewed in reference 26). As such, proper regulation of the CED-3/ICE-like proteases is critical for execution or prevention of cellular apoptotic death.

A variety of viruses induce apoptosis within their host cell by mechanisms that are not fully understood (reviewed in reference 35). To counter this apparent antiviral defense by the host, viruses express diverse genes with antiapoptotic activity. This viral strategy can enhance virus multiplication or establish viral persistence and latency and thus contributes to virus survival (6, 9, 12, 15, 25, 33). Virus intervention in the host apoptotic response has been used to define critical steps in the pathway since viral antiapoptotic proteins mimic or regulate conserved components of the death program. For example, the adenovirus E1B 19K (5, 33), Epstein-Barr virus BHRF1 (15), and African swine fever virus LMW5-HL (28) proteins are homologous to the products of the programmed cell death suppressor genes *bcl-2* and *ced-9* from mammals and *C. elegans*, respectively (for recent reviews, see references 16, 22, 43, 45). In the case of adenovirus E1A-induced apoptosis, stable expression of E1B 19K prevents apoptosis as well as processing of the zymogen form of CED-3/ICE protease CPP32 that occurs upon adenovirus infection (2). Thus, like *ced-9*, E1B 19K may regulate programmed cell death upstream from *ced-3*/*ice*. In a separate strategy that may also prevent *ced-3*/*ice* function, the cowpox virus *crmA* gene (SPI-2) encodes a serpin-like protein capable of direct inhibition of specific ICE-related proteases (34, 38, 39, 44).

The baculovirus gene *p35* is a general and effective suppressor of programmed cell death. Upon viral or cellular expression, *p35* blocks baculovirus-induced apoptosis and restores virus replication (4, 6, 7, 17). Suggestive of inhibition at a highly conserved step in the death pathway, *p35* expression not only suppresses apoptosis in uninfected lepidopteran cells (4, 8) but also prevents developmental programmed cell death in *C. elegans* (37) and *Drosophila melanogaster* (13, 14), blocks neuronal cell death (27, 32), and suppresses tumor necrosis factor- and Fas-induced death of mammalian cells (1). Consistent with its effectiveness in diverse organisms, it was recently demonstrated that the *p35* gene product (P35) is a potent inhibitor of CED-3/ICE-related proteases, including human ICE, ICH-1, ICH-2, CPP32, and *C. elegans* CED-3 (3, 46). Thus, these studies suggested that P35 prevents programmed cell death by inhibiting the CED-3/ICE-related proteases. Although CED-3/ICE protease-mediated cleavage at P35 Asp-87–Gly-88 is involved, both irreversible (3) and competitive (46) mechanisms for P35 inhibition have been proposed.

To examine the molecular mechanism by which P35 prevents apoptosis in the baculovirus-infected cell, the natural context in which P35 evolved, we have used a combination of genetic and biochemical approaches that identified protein domains

* Corresponding author. Present address: Bock Laboratories, 1525 Linden Dr., Madison, WI 53706-1596. Phone: (608) 262-7774. Fax: (608) 262-7414. Electronic mail address: PFriesen@facstaff.wisc.edu.

† Present address: Laboratory of Clinical Investigation, National Institutes of Health, Bethesda, MD 20892.

required for P35 function and protein interaction. We report here that during infection of *Spodoptera frugiperda* SF21 cells with the prototype baculovirus *Autographa californica* nuclear polyhedrosis virus (Ac*M*NPV), a novel CED-3/ICE-like protease (*Sf* protease) is activated. The protease(s) cleaves P35 and is potently inhibited by P35. In vitro inhibition of *Sf* protease activity by recombinant P35 was abolished by amino acid substitutions within the P35 cleavage site, including the P_1 and P_4 Asp residues adjacent to the scissile peptide bond. Moreover, the P_1 and P_4 mutations disrupted P35 antiapoptotic activity in virus-infected cells. Collectively, these results support the hypothesis that P35 blocks virus-induced apoptosis by inhibiting a virus-activated CED-3/ICE-like protease through a mechanism that includes protease interaction and P35 cleavage. The induction of the *Sf* protease and its subsequent inhibition by viral synthesized P35 further suggest that virus-mediated signals which trigger apoptosis must function upstream from *ced-3*/*ice* in the death program.

MATERIALS AND METHODS

Cells and viruses. *S. frugiperda* IPL-SF21 cells (42) and *Trichoplusia ni* TN368 cells (19) were propagated at 27°C in TC100 growth medium containing 10% fetal bovine serum and 2.6% tryptose broth. Cell monolayers were inoculated (time zero) with extracellular, budded virus at a multiplicity of infection (MOI) of 10 to 20 PFU per cell. Ac*M*NPV recombinants (L1 strain) with a wild-type or mutated copy of *p35* inserted at the polyhedrin locus were constructed by gene replacement as described previously (17). The genotype of plaque-purified mutants was verified by restriction analysis of isolated viral DNA or PCR-amplified DNA fragments containing *p35*. Ac*M*NPV recombinants vΔ35K, vΔ35K/lacZ/-35K$^+$, and vΔ35K/lacZ were described previously (17, 18).

***p35* mutagenesis.** Oligonucleotide site-directed mutagenesis (21) was performed by using plasmid p35KORF-hr5$^+$ (18). Two-codon (Ala-Ser) insertion oligonucleotides contained an *Nhe*I site (GCTAGC) and ranged in size from 30 to 41 nucleotides. Oligonucleotides in which acidic and basic residues were replaced with alanine, i.e., charged-to-alanine substitutions (ca) (underlined), are shown below: ca17, 5′-GTTTGTCCACCTGGCATGCAGCAATAATCGTCTGGG-3′; ca26, 5′-GTTAATGTACACCAAAGCCGCGGTTTGTTTGTCCA-3′; ca58, 5′-GCGCAAATTGTTGTTAGCAGCTGTAACGCTTCGTAT-3′; ca64, 5′-CATCGACTTTTGATTTTTATAGCTGCAGCCAAATTGTTGTTCTTG-3′; ca70, 5′-CGCGACAGAATAAAAAGCGCTGTCGCGGCGCAATTTGATCAACTA-3′; ca79, 5′-CATTTGATCGCTGTAAGCTGCAGTAGTTGATCAAATTG-3′; ca84, 5′-CGCGATTACAGCGCTCAAATGGATGGATTC-3′; ca87, 5′-TACAGCGATCAAATGGCCGGCT TCCACGATAGCATC - 3′; ca90, 5′-TTTAAAATACTTGATGCTAGCAGCGAATCCATCCATTTG-3′; ca97, 5′-CTTACCGAATAGTGAGCTGCAGCAAAATACTTGATGCTATC-3′; ca112, 5′-GACTCTTTAAAATTTTAGCAAAAGCGCTAGCCAACACGC TGCCATT-3′; ca126, 5′-GTAAGCTTCAATAGAAGCTGCAGCGGTATAATCATGACT-3′; ca143, 5′-ACGTAGTAGTCGTTAGCTGCAGCGACCAATTTGGGC-3′. Oligonucleotides encoding the influenza virus hemagglutinin (HA) epitope YPYDVPDYA were inserted into *Nhe*I sites of p35KORF-hr5$^+$ at codons 174 and 205. All mutations were confirmed by restriction analysis and DNA sequencing.

Marker rescue, DNA fragmentation, and β-galactosidase assays. SF21 cells were transfected in triplicate with two or three independently isolated *p35*-containing p35KORF-hr5$^+$ plasmids by using Lipofectin (Bethesda Research Laboratories). Transfected cells were infected 16 h later with vΔ35K/lacZ (MOI of 0.5). Extracellular virus was harvested 3 days later and quantified by plaque assay using SF21 cells and 100 μg of X-Gal (5-bromo-4-chloro-3-indolyl-β-D-galactopyranoside) per ml of agarose overlay. Low-molecular-weight DNA was isolated from SF21 cells, combined with any associated apoptotic bodies, and subjected to agarose gel electrophoresis (18). Intracellular β-galactosidase activity was determined as described previously (17).

Immunoblot analysis. Immunoblots of freeze-thaw or total cell lysates were incubated for 1 h with a 1:2,500 to 1:10,000 dilution of α-P35NF polyclonal antisera, followed by a 1:2,500 to 1:10,000 dilution of goat anti-rabbit immunoglobulin G (IgG) (Pierce) conjugated to alkaline phosphatase. α-P35NF was derived from P35 residues 43 to 132 synthesized as a TrpE fusion protein in *Escherichia coli* (17). HA epitope-containing P35 was detected by using a 1:1,000 dilution of HA-specific 12CA5 mouse monoclonal antibody (BAbCO) and a 1:10,000 dilution of goat anti-mouse IgG (Jackson ImmunoResearch Laboratories, Inc.) conjugated to alkaline phosphatase. Color development was as described previously (18).

Pulse-chase and immunoprecipitation analyses. The growth medium from SF21 cells infected 12 h previously (MOI of 20) was replaced with phosphate-buffered saline containing 200 μCi of Tran^{35}S-Label (>1,000 Ci/mmol; ICN Biomedicals, Incorp.) per ml. After 30 min, the radiolabel was replaced with medium containing a 50-fold excess of unlabelled methionine and cysteine. Cells were collected, washed, and suspended in lysis buffer (50 mM Tris [pH 8.0], 50 mM KCl, 0.2% Nonidet P-40). After 30 min on ice, the resulting lysates were clarified by centrifugation (14,000 × *g*) and frozen. For immunoprecipitations, cell lysates were diluted 1:10 with buffer 10 (60 mM Tris [pH 7.4], 50 mM KCl, 2 mM benzamidine, 0.2% Triton X-100), and incubated with 12CA5 serum for 2 h at 6°C. The immune complexes were collected with protein A-Sepharose beads, washed three times with buffer 10, and eluted by boiling in 1% sodium dodecyl sulfate (SDS)–2.5% β-mercaptoethanol. Immunoprecipitated proteins were subjected to SDS-polyacrylamide gel electrophoresis and fluorography (En^{3}Hance; DuPont).

Protease expression. To prepare *Sf* protease-containing extracts, SF21 cells were collected 24 h after infection and suspended in a solution of 10 mM HEPES (*N*-2-hydroxyethylpiperazine-*N*′-2-ethanesulfonic acid) (pH 7.0), 0.1% CHAPS {3-[(3-cholamidopropyl)-dimethyl-ammonia]-1-propanesulfonate}, 5 mM dithiothreitol, and 2 mM EDTA that contained protease inhibitor cocktail (Pharmingen). After one freeze-thaw cycle, the cells were subjected to Dounce homogenization. Cell lysates were clarified by centrifugation (150,000 × *g*) for 2 h and stored at −80°C. Recombinant human CPP32 (hCPP32) and mouse ICE (mICE) were expressed in *E. coli* BL21(DE3) by using plasmid pET3a or pET-21b (Novagen) containing *Nde*I-*Bam*HI and *Bam*HI-*Xho*I fragments of the mICE or hCPP32 cDNA, respectively. *E. coli* cultures at an optical density at 600 nm of 1.0 were induced by IPTG (isopropyl-β-D-thiogalactopyranoside) (1 mM final concentration) and shaken for 3 h at 25°C. Cells were collected and suspended in ice-cold 50 mM Tris (pH 8.0)–5 mM EDTA–50 mM KCl. After sonication, the lysate was clarified by centrifugation (30,000 × *g*) for 30 min (4°C) and stored. mICE and hCPP32 concentrations were determined by stoichiometric titration with Ac-YVAD-chloromethylketone and Ac-DEVD-CHO, respectively (30).

IVT P35 cleavage assays. The SP6 promoter-containing plasmid pSP35K was generated by inserting a 1,096-bp *Nru*I-*Eco*RI *p35* fragment into *Hin*cII and *Eco*RI sites of pSP64 (Promega Corp.). *p35* mutations D84A, D87A, and H90A-D91A were introduced by subcloning. Coupled transcription-translation reactions were conducted by using rabbit reticulocyte lysates and Tran^{35}S-Label as specified by the manufacturer of the TNT system (Promega Corp.). Protease-containing cell extracts were incubated for 30 min with or without inhibitors and then mixed with radiolabeled in vitro-translated (IVT) P35 (0.5 μl); inhibitors included aprotinin (2 μg/ml), leupeptin (100 μM), pepstatin A (1 μM), E64 (100 μM), EDTA (5 mM), iodoacetate (1 μM), phenylmethylsulfonyl fluoride (1 μM), and the acetyl-tetrapeptides Ac-DEVD-CHO and Ac-YVAD-CHO (10 μM). All reaction mixtures (20 μl) contained 100 mM HEPES (pH 7.5), 2 mM dithiothreitol, 0.1% CHAPS, and 10% sucrose. After a 2-h incubation (30°C), the reactions were terminated by boiling and mixtures were subjected to electrophoresis on 5 to 20% polyacrylamide gradient gels and fluorography.

Purification of recombinant P35-His$_6$ and protease inhibition assays. *p35* was inserted into *Nde*I and *Not*I sites of pET-22b(+) to generate plasmid pP35-C(His$_6$); all mutations were introduced by subcloning. Overexpression in *E. coli* strain BL21(DE3) yielded protein P35-His$_6$ with a C-terminal extension (A$_3$LEH$_6$). *E. coli* extracts were mixed with Ni^{2+}-charged His-Bind resin (Novagen) in binding buffer (20 mM Tris [pH 7.9], 5 mM imidazole, 0.5 M NaCl). The resin was washed with 30 mM imidazole-containing binding buffer and bound protein was eluted with an equal volume of 100 mM imidazole-containing binding buffer. After dialysis into phosphate-buffered saline, concentrations were determined by the bicinchoninic acid method (Pierce) for wild-type (1.75 mg/ml) and D87A (0.71 mg/ml)-, D84A (1.1 mg/ml)-, and H90A-D91A (1.3 mg/ml)-mutated P35-His$_6$ proteins. The resulting P35-His$_6$ proteins were >95% pure, as judged by polyacrylamide gel electrophoresis.

For protease inhibition assays, serial dilutions of P35-His$_6$ in 50 μl of assay buffer (25 mM HEPES [pH 7.5], 1 mM EDTA, 2 mM dithiothreitol, 0.1% CHAPS, 10% sucrose) were mixed with an equal volume of protease-containing assay buffer. After 30 min at room temperature, a 20 μM stock of the acetyl-tetrapeptide amino-4-methylcoumarin substrate Ac-DEVD-amc or Ac-YVAD-amc in assay buffer was added, giving a final substrate concentration of 10 μM. Fluorescent product accumulation (excitation, 360 nm; emission, 460 nm) was measured in a Cytofluor II plate reader (Millipore Corp.). Fifty percent inhibitory concentrations (IC$_{50}$s) were calculated by using single time point measurements taken during linear product release within the first 10% of each reaction.

RESULTS

P35 contains multiple functional domains. P35 bears no obvious sequence similarity to known death regulators. Thus, to identify protein domains required for suppression of apoptosis in invertebrate cells, we first constructed a series of in-frame, two-codon (Ala-Ser) insertions throughout *p35*. An effort was made to target those residues within or near domains predicted by computer algorithm to form regions of secondary structure. The effect of these mutations on *p35*'s capacity to restore replication of an Ac*M*NPV *p35* null mutant by blocking virus-induced apoptosis was measured by marker rescue. In this assay, genomic integration of functional *p35*

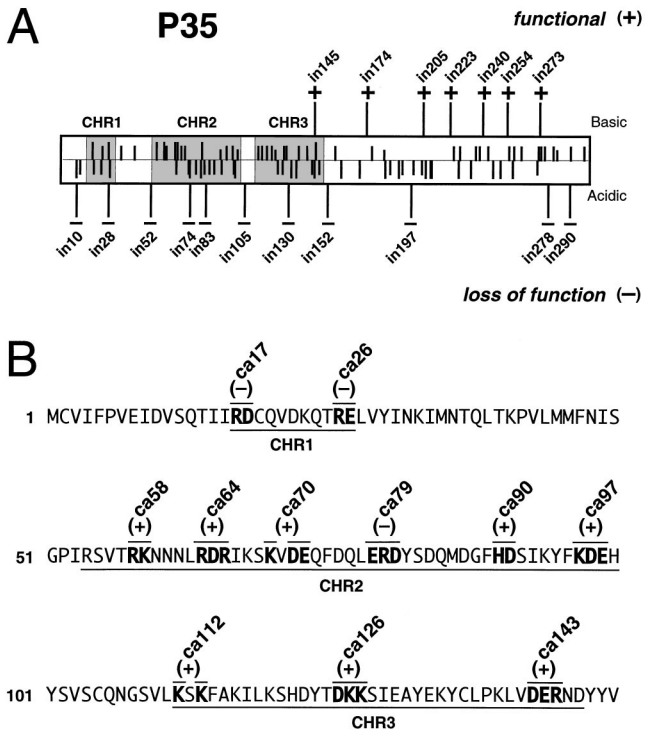

FIG. 1. Marker rescue analysis of *p35* mutations. (A) Ala-Ser insertions (in). Vertical bars above or below P35 (open box) denote Ala-Ser insertions, designated by the position of the amino acid preceding the insertion. Mutations were assayed by marker rescue in which the replication of *p35*-deletion mutant vΔ35K/lacZ was restored upon integration of a functional copy of *p35*. Yields of rescued, *lacZ*-expressing ($p35^+$) virus were measured by plaque assay using apoptosis-sensitive SF21 cells. Vertical bars below P35 depict insertions that caused loss of function (−), defined as <500 blue PFU recovered per ml, whereas bars above P35 depict insertions that had no effect (+), defined as >37,000 blue PFU per ml. Charged regions CHR1, CHR2, and CHR3 (shaded boxes) are shown with acidic (down) or basic (up) residues as thin lines. (B) ca mutations. Each substitution (overlined) is designated by the position of the first altered residue. Mutations that caused *p35* loss of function as determined by marker rescue (<10 blue PFU per ml) are indicated by the "(−)", whereas mutations that had no effect (>37,000 blue PFU per ml) are indicated by the "(+)". CHR1, CHR2, and CHR3 are underlined.

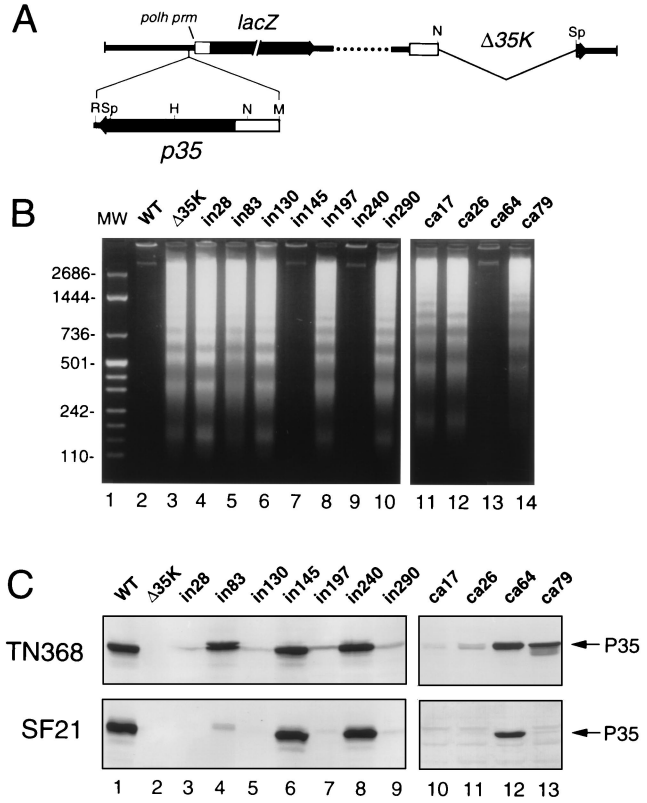

FIG. 2. Suppression of virus-induced apoptosis by Ac*M*NPV *p35* mutants. (A) Gene organization of *p35* mutants. For all viral mutants, *p35* (shaded arrow) under control of its own promoter (open box) and the adjacent *lacZ* reporter gene were inserted at the polyhedrin locus of a *p35*-deletion mutant vΔ35K (17); *lacZ* expression was directed by the very late polyhedrin promoter (polh prm). Restriction site abbreviations: H, *Hin*dIII; M, *Mlu*I; N, *Nru*I; R, *Eco*RI; Sp, *Spe*I. (B) p35-mutant-induced intracellular DNA fragmentation. Low-molecular-weight DNA was extracted from SF21 cells and associated apoptotic bodies 34 h after infection with viruses containing the indicated *p35* mutations and subjected to agarose gel electrophoresis in the presence of ethidium bromide. DNA from cells infected with wild-type *p35*-containing vΔ35K/lacZ/$35K^+$ (WT) or *p35*-deletion mutant vΔ35K/lacZ (Δ35K) was included, along with DNA molecular weight (MW) markers. (C) Intracellular P35 accumulation. TN368 and SF21 cells were harvested 24 h after infection with viruses containing the indicated *p35* mutations. SDS-cell lysates (4×10^5 cell equivalents per lane) were subjected to gel electrophoresis and immunoblot analysis by using α-P35NF serum.

plasmids restored replication of the Ac*M*NPV *p35* deletion mutant vΔ35K/lacZ (17), as indicated by the appearance of *lacZ*-expressing, blue viral plaques upon infection of apoptosis-sensitive SF21 cells. Transfection of plasmids containing wild-type *p35* typically yielded 30,000 to 70,000 rescued plaques per ml of growth medium, whereas plasmids lacking *p35* yielded fewer than 10 plaques per ml.

Eleven of eighteen Ala-Ser insertions caused *p35* loss of function (Fig. 1A). Only seven insertions, all within the C-terminal half of P35, had no effect compared with that of wild-type *p35*. None of the insertions had an intermediate rescue phenotype, since there was at least a 750-fold difference in the yield of virus obtained by using functional *p35* compared with nonfunctional *p35*. Two Ala-Ser insertions (in278 and in290) near the C terminus caused loss of function, confirming the importance of this region for P35 function (17). Most notable was the overall sensitivity of the N-terminal half of P35 to insertional mutagenesis, where eight of nine mutations in the first 152 residues caused loss of function.

To further define functional domains within the N-terminal half of P35, we constructed a series of clustered ca mutations in which acidic and basic residues were substituted with Ala (Fig. 1B). Since clusters of charged residues often reside on the solvent-exposed surface of the protein, it was presumed that replacement of such residues would disrupt electrostatic interactions with other proteins while having a minimal effect on protein stability. Thus, three charged regions, CHR1, CHR2, and CHR3, within the N-terminal half of P35 were targeted (Fig. 1B). As determined by marker rescue, charged-to-alanine mutations ca17 and ca26 within CHR1, and ca79 within CHR2, caused *p35* loss of function. In contrast, mutations ca58, ca64, ca70, ca90, and ca97 within CHR2, and all CHR3 mutations (ca112, ca126, and ca143), had no effect on *p35* function. Thus, charged residues within CHR1 and CHR2, but not CHR3, were critical for P35 function.

***p35* marker rescue loss-of-function mutations fail to block apoptosis.** To assess the nature of the *p35* defects, we constructed Ac*M*NPV recombinants in which mutated forms of *p35* were introduced along with the *lacZ* reporter gene into the genome of a *p35*-deletion mutant (Fig. 2A). Such recombinants provided an effective means for discerning effects on P35 function and stability. Since Ac*M*NPV-induced apoptosis of

TABLE 1. β-Galactosidase activity of Ac*M*NPV recombinants expressing mutated *p35*

Virus	β-Galactosidase activity (A_{420}/min/10^6 cells)[a]		SF/TN activity[b] (%)
	SF21	TN368	
Wild-type *p35*	38.7 ± 4.7	60.0 ± 4.8	100
p35$^-$	0.040	62.9 ± 7.6	0.09
in28	0.031	52.8 ± 6.8	0.08
in83	0.083	51.3 ± 1.8	0.24
in130	0.024	42.7 ± 6.1	0.09
in145	26.0 ± 14	59.6 ± 10	66
in197	0.033	50.7 ± 8.5	0.10
in240	27.0 ± 13	68.2 ± 13	61
in290	0.072	71.9 ± 7.8	0.15
ca17	0.041	184 ± 13	0.03
ca26	0.034	37.8 ± 7.3	0.14
ca64	39.6 ± 9.5	30.4 ± 9.9	200
ca79	0.038	35.1 ± 7.7	0.17

[a] Intracellular β-galactosidase activity was determined 48 h after infection (MOI of 5). Values shown are averages (± standard deviations) from infections performed in triplicate by using two independently isolated Ac*M*NPV recombinants as indicated.

[b] The SF/TN activity ratio was calculated by normalizing the ratio of β-galactosidase activity in SF21 cells relative to TN368 cells for a particular virus to that obtained in cells infected with wild-type *p35*-containing virus vΔ35K/lacZ/35K$^+$.

SF21 cells is characterized by intracellular DNA fragmentation accompanied by membrane blebbing and cytolysis (6, 17), the ability of each mutant to suppress apoptosis was first assessed by measuring the level of intracellular DNA fragmentation (Fig. 2B). Each of the marker rescue loss-of-function mutations tested (in28, in83, in130, in197, in290, ca17, ca26, and ca79) failed to suppress virus-induced DNA fragmentation. Low-molecular-weight DNA levels in cells infected by these *p35* mutants were comparable to that in cells infected by *p35*-deletion mutant vΔ35K/lacZ (Fig. 2B, lane 3). In contrast, mutations that had no effect on *p35* function (in145, in240, and ca64) suppressed DNA fragmentation as effectively as wild-type *p35*-containing vΔ35K/lacZ/35K$^+$ (Fig. 2B, lane 2).

All *p35* mutants defective for apoptotic suppression failed to support virus late gene expression. Expression of *lacZ* under control of the very late polyhedrin promoter (Fig. 2A) was used as an indicator of *p35* function, since very late gene expression is restricted in SF21 cells but not apoptosis-resistant TN368 cells infected with *p35* null mutants (13). All mutations that were functional by marker rescue produced β-galactosidase at levels comparable to that of wild-type *p35* (Table 1). The *p35* loss-of-function mutants tested produced little or no β-galactosidase in SF21 cells but produced normal levels in TN368 cells (SF21/TN368 ratios ranging from of 0.03 to 0.24%). None of the *p35* mutations that exhibited wild-type antiapoptotic activity were defective for late gene expression or virus replication. This finding is consistent with the hypothesis that suppression of apoptosis is *p35*'s primary function during infection.

In some cases, *p35* loss-of-function mutations affected the in vivo stability of P35. As determined by immunoblot assays (Fig. 2C), viruses expressing functional *p35* (in145, in240, and ca64) produced steady-state levels of P35 comparable to that of wild-type P35, in both TN368 and SF21 cell lines. In contrast, little, if any P35 was detected in SF21 cells infected with loss-of-function mutants in28, in130, in197, in290, ca17, and ca26 (Fig. 2C). Lack of P35 detection was likely due to the absence of protein and not to diminished recognition by α-P35NF antiserum, which was generated against P35 residues 43 to 132 (18). Although the mutated P35s were detected in nonapoptotic TN368 cells, accumulation was reduced. However, the near-wild-type accumulation of loss-of-function mutations in83 and ca79 in TN368 cells (Fig. 2C, lanes 4 and 13) suggested that these CHR2 residues have little effect on P35 stability.

P35 is proteolytically cleaved within CHR2 during infection. The overall sensitivity of CHR1 and CHR2 to mutagenesis was consistent with a role of the N terminus of P35 in mediating protein-protein interactions required for function. To examine these interactions in infected cells, we first epitope-tagged P35 at a position distal to the N-terminal charged domains (Fig. 3A) and constructed Ac*M*NPV recombinants. As predicted from Ala-Ser mutagenesis (Fig. 1A), insertion of the influenza HA epitope at residue 174 or 205 had a minimal effect on P35 function as judged by the capacity of P35^{HA174} and P35^{HA205} to block apoptosis (see below). By using HA-specific monoclonal serum, immunoblots of intracellular proteins from recombinant virus-infected cells revealed full-length P35^{HA205} (~40 kDa) and a predominant, smaller (~29 kDa) HA-tagged protein (Fig. 3B). Whereas P35^{HA205} appeared by 4 h and accumulated through 24 h after infection, the 29-kDa protein did not appear until 10 h. The later appearance and parallel accumulation of the smaller protein suggested that it was derived by proteolytic cleavage of full-length P35.

Pulse-chase analyses conducted during the peak of P35 synthesis (12 h after infection) demonstrated that P35 was cleaved to produce the smaller fragment (Fig. 3C). Immunoprecipitable P35^{HA174} and P35^{HA205} decreased during the 9-h chase, whereas the corresponding HA-cleavage fragment increased concomitantly; the electrophoretic mobility of HA-tagged proteins and their respective cleavage fragment varied, depending on the location of the epitope. Full-length P35^{HA174} disappeared during the chase, exhibiting a half-life of 1 h or less. Although P35^{HA205} may have a similar half-life, its turnover was obscured by a comigrating protein (Fig. 3C, lanes 8 to 13) that accumulated during the chase; the origin of this protein is unknown. On the basis of the size of the largest fragment and the position of the HA epitope, P35 was proteolytically cleaved within CHR2. The untagged 10-kDa sister fragment derived from the N terminus was not detected (see below). Moreover, the polyclonal antiserum α-P35NF failed to detect either P35 fragment, suggesting that P35 cleavage is accompanied by a change in protein conformation.

Asp-87 is required for P35 cleavage and suppression of virus-induced apoptosis. The finding that P35 is cleaved during infection indicated that P35 can function as a substrate in vivo. Since recombinant CED-3/ICE proteases cleave P35 at Asp-87–Gly-88 (3, 46), we replaced Asp-87 with Ala (D87A) (Fig. 4A) to verify cleavage at the P_1 position and to determine the significance of cleavage with respect to P35 antiapoptotic activity. An Ac*M*NPV recombinant (ca87^{HA}) in which D87A was inserted within HA205-tagged *p35* was constructed. Whereas cleavage of wild-type P35^{HA205} was readily detected in SF21 cells (Fig. 4B, lanes 1 to 4), D87A abolished cleavage (lane 6). Accumulation of intracellular P35(D87A) was reduced approximately 20-fold relative to wild-type P35; this reduction was attributed to premature, apoptotic death of ca87^{HA}-infected cells since mutant and wild-type protein levels were indistinguishable in infected, nonapoptotic TN368 cells (data not shown). The elimination of P35(D87A) cleavage was accompanied by loss of P35 antiapoptotic activity, since marker rescue assays demonstrated that P_1(D87A)-substituted *p35* was nonfunctional (Fig. 4A). Moreover, infection assays using mutant ca87^{HA} indicated that P35(D87A) failed to suppress DNA

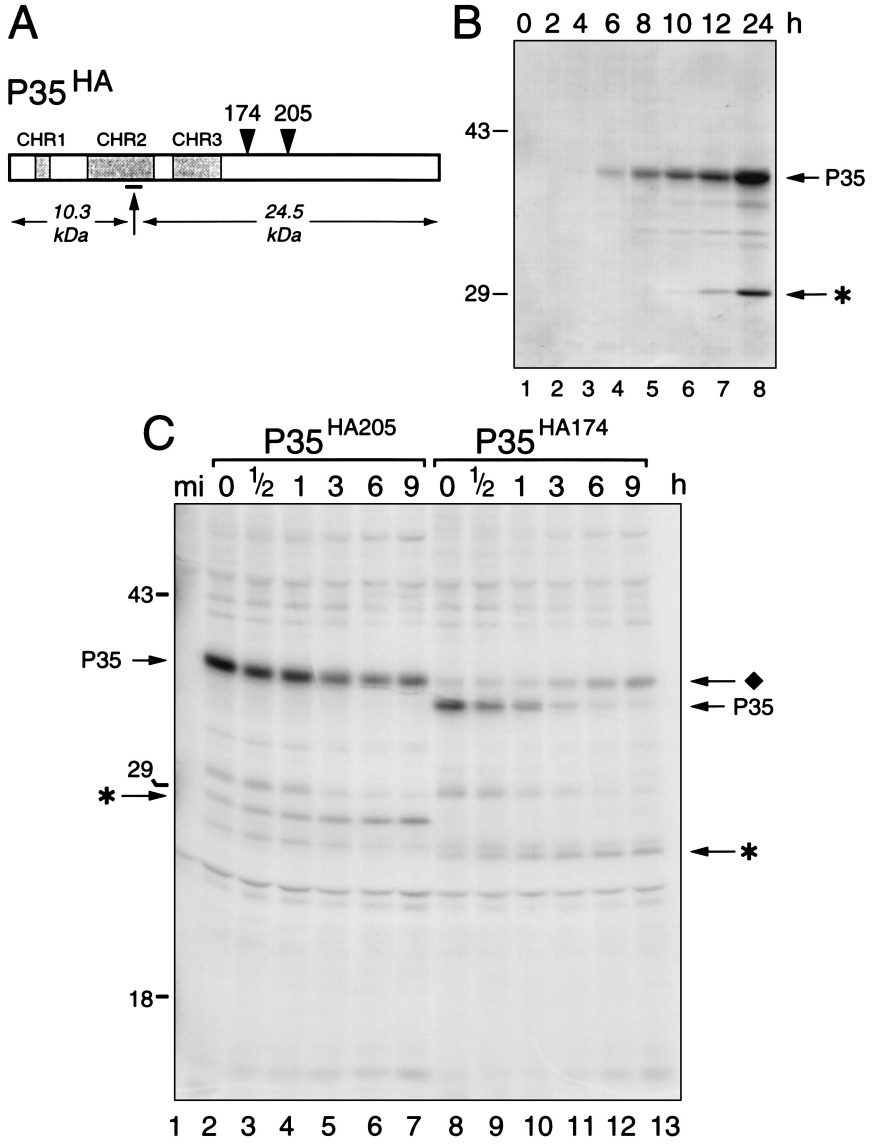

FIG. 3. Proteolytic cleavage of P35 during baculovirus infection. (A) $P35^{HA}$ of Ac*M*NPV recombinants. The nine-residue HA epitope was introduced into P35 (open box) at residue 174 or 205. The vertical arrow denotes the site of P35 cleavage within CHR2, generating ~10- and ~25-kDa fragments. (B) Immunoblot analysis of intracellular P35. SF21 cells were harvested at the indicated times (h) after infection with vΔ35K/lacZ/$p35^{HA205}$. SDS-cell lysates (5×10^5 cell equivalents per lane) were subjected to immunoblot analysis by using HA-specific 12CA5 monoclonal serum. Uncleaved $P35^{HA205}$ and the cleaved HA-containing 29-kDa fragment (*) are indicated. The positions of molecular size standards (in kilodaltons) are shown. (C) Pulse-chase analysis. SF21 cells were radiolabeled for 30 min with Tran^{35}S-Label 12 h after infection with vΔ35K/lacZ/$p35^{HA205}$ (lanes 2 to 7) or vΔ35K/lacZ/$p35^{HA174}$ (lanes 8 to 13). Cell lysates were prepared at the indicated times (h) during the chase period, immunoprecipitated (5×10^5 cell equivalents) by using 12CA5 serum, and subjected to polyacrylamide gel electrophoresis and fluorography. Mock-infected (mi) SF21 cells were analyzed similarly (lane 1). Uncleaved $P35^{HA205}$ and $P35^{HA174}$, the largest HA-containing P35 cleavage product (*), and the larger-than-P35 protein (diamond) are indicated. Molecular size standards (in kilodaltons) are on the left.

fragmentation and membrane blebbing, which were comparable to that of *p35*-deletion mutant vΔ35K/lacZ (Fig. 4C).

Asp-84 is required for P35 apoptotic suppression but not proteolytic cleavage. Since the P_4 residue at the cleavage site can also affect substrate proteolysis by ICE (reviewed in reference 41), P35 Asp-84 was replaced with Ala and introduced into an Ac*M*NPV recombinant ($ca84^{HA}$). Cleavage of P35(D84A) was readily detected in infected cells (Fig. 4B, lane 7). Accumulation of P35(D84A) was reduced in apoptotic SF21 cells but not in nonapoptotic TN368 cells (data not shown), suggesting that Asp-84 had little effect on P35 stability. Despite its cleavage, P35(D84A) failed to prevent virus-induced apoptosis, as indicated by marker rescue and independent assays with mutant $ca84^{HA}$ (Fig. 4A and C). Constructed *p35* mutant $ca79^{HA}$ in which residues 79 to 81 were replaced with alanines (Fig. 4A) also failed to prevent apoptosis (Fig. 4C), even though cleavage of intracellular P35($ca79^{HA}$) was detected (Fig. 4B, lane 8). Accumulation of P35(ca79) was also reduced in apoptotic SF21 but not in TN368 cells (Fig. 2C). These data indicated that residues N terminal to the P35 scissile bond affect antiapoptotic activity, despite P35 cleavage.

Wild-type P35, but not P_1-mutated P35, is a substrate for a virus-induced CED-3/ICE-like protease. The Asp-87 dependency of P35 cleavage suggested that baculovirus infection directly or indirectly activates a CED-3/ICE-related protease. To test this possibility, cytosolic extracts were prepared from

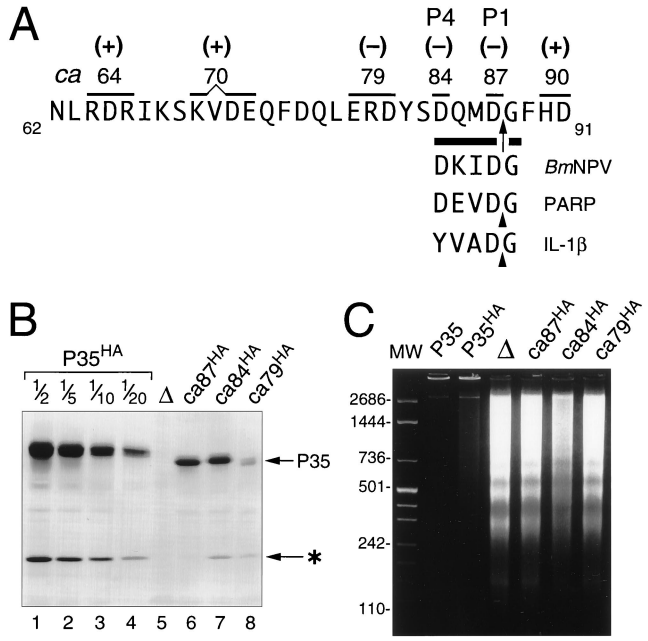

FIG. 4. Role of Asp-87 and Asp-84 in P35 cleavage and apoptotic suppression. (A) ca mutagenesis. The indicated alanine substitutions (overlined) were assayed by marker rescue and scored as functional [(+)] or loss of function [(−)], as described in the legend to Fig. 1. P_4 to P_1' residues of P35 from *Bombyx mori* nuclear polyhedrosis virus (*Bm*NPV) (20), poly(ADP-ribose) polymerase (PARP) (24), and pro-interleukin-1β (IL-1β) (41) are also shown; cleavage occurs between Asp (P_1) and Gly (P_1'). (B) P35 proteolytic cleavage. Lysates (5×10^5 cell equivalents) from SF21 cells 24 h after infection with viruses expressing the indicated mutations of $p35^{HA205}$ (lanes 6 to 8) or vΔ35K/lacZ (lane 5) were subjected to immunoblot analysis using HA-specific 12CA5 serum. Serial twofold dilutions of wild-type $P35^{HA205}$-containing lysate were included (lanes 1 to 4). *, largest HA-containing P35 cleavage product. (C) Intracellular DNA fragmentation. Low-molecular-weight DNA was extracted from SF21 cells 24 h after infection with vΔ35K/lacZ/$35K^+$ (P35), vΔ35K/lacZ/$p35^{HA205}$ ($P35^{HA}$), vΔ35K/lacZ (Δ), or viruses containing the indicated $p35^{HA205}$ mutations and analyzed as described in the legend to Fig. 2B. MW, molecular weight standards.

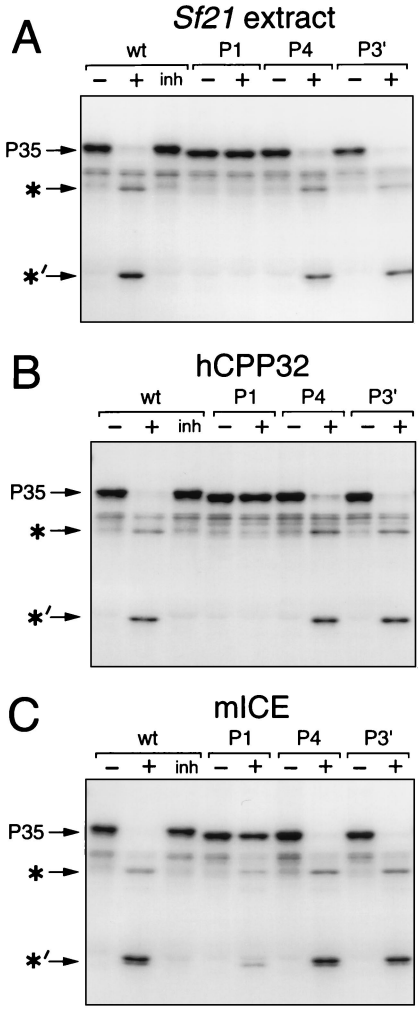

FIG. 5. Cleavage of IVT P35 by ICE-related proteases. [^{35}S]Met-Cys-labeled wild-type (wt) P35 or P35 that contained D87A (P_1), D84A (P_4), or H90A-D91A (P_3') mutations was mixed with (+) or without (−) cytosolic extracts of apoptotic vΔ35K-infected SF21 cells (A) or with *E. coli* extracts containing either hCPP32 (B) or mICE (C). Where indicated, the tetrapeptide aldehyde inhibitor (inh) acetyl-DEVD-CHO was included in reactions with hCPP32 and SF21 extracts, while acetyl-YVAD-CHO was included with mICE. After 2 h, the reactions were terminated and subjected to polyacrylamide gel electrophoresis and fluorography. Full-length P35 and the 25-kDa (*) and 10-kDa (*′) cleavage fragments are indicated.

apoptotic SF21 cells infected with the *p35* null mutant vΔ35K. Incubation of these extracts with IVT wild-type P35 yielded 10- and 25-kDa fragments (Fig. 5A), indicative of cleavage at Asp-87–Gly-88 (3, 46). Due to its fivefold higher methionine content, the 10-kDa fragment exhibited greater radiolabeling than the 25-kDa fragment. Indicating the requirement for P35 Asp-87, the virus-induced SF21 protease activity (*Sf* protease) cleaved P_4(D84A)- and P_3'(H90A-D91A)-mutated P35 but not P_1(D87A)-mutated P35 (Fig. 5A). IVT P35 was cleaved similarly by recombinant hCPP32 and mICE (Fig. 5B and C). Since P_1-mutated P35 was resistant to cleavage but P_4- and P_3'-mutated P35 were not, these ICE-related proteases exhibited a P35 substrate specificity similar to that of the *Sf* protease.

The appearance of the *Sf* protease activity was correlated with apoptosis since this IVT P35-cleaving activity was only detected in extracts from SF21 cells infected with *p35* null mutants, not from mock-infected or wild-type *p35* virus-infected cells (Fig. 6, lanes 1 to 3). An identical proteolytic activity was detected in extracts of SF21 cells induced to undergo apoptosis by exposure to the transcription inhibitor actinomycin D (22a). These findings suggested that the *Sf* protease is host encoded and is activated upon apoptotic signaling.

To characterize the mechanistic properties of the virus-induced *Sf* protease, various inhibitors were tested. Serine-, metallo-, and aspartic-protease inhibitors failed to block cleavage of IVT P35 by the *Sf* protease activity (Fig. 6, lanes 4 to 8). The alkylating agent iodoacetate, but not the cysteine protease inhibitor E64, blocked cleavage (lanes 9 and 10). The tetrapeptide aldehyde Ac-DEVD-CHO, a potent inhibitor of CPP32 and MCH3 (11, 29), also inhibited cleavage (lane 11). In contrast, the ICE-selective inhibitor Ac-YVAD-CHO (41) had little effect at comparable concentrations (lane 12). Instead, Ac-YVAD-CHO blocked IVT P35 cleavage by mICE (Fig. 5C). Cleavage of IVT P35 by hCPP32 exhibited a quantitatively similar sensitivity to Ac-DEVD-CHO and reduced sensitivity to Ac-YVAD-CHO (Fig. 5B and data not shown). Collectively, these findings indicated that the apoptosis-associated *Sf* protease activity involved an invertebrate member of the CED-3/ICE family of proteases with a substrate specificity more closely resembling that of CPP32 and MCH3 than ICE.

Recombinant P35-His_6 inhibits virus-induced *Sf* and mammalian ICE-related proteases. The cleavage of de novo-syn-

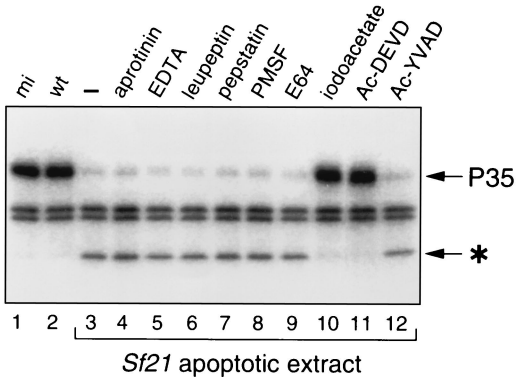

FIG. 6. Inhibition of P35 cleavage activity from apoptotic SF21 cells. Cytosolic extracts prepared from cells that were mock infected (mi) or infected with wild-type (wt) or *p35* deletion (vΔ35K) viruses were incubated alone (−) or in the presence of the indicated inhibitor for 15 min and then mixed with IVT P35. After 2 h, the reactions were subjected to gel electrophoresis and fluorography. Full-length P35 and the larger, 25-kDa cleavage fragment (*) are indicated. PMSF, phenylmethylsulfonyl fluoride.

thesized P35 by a baculovirus-induced CED-3/ICE-like activity suggested that P35 prevents host cell apoptosis by protease inhibition. Thus, the abilities of wild-type and mutated P35 to inhibit the *Sf* protease were determined. P35 was His_6-tagged at its C terminus (P35-His_6), overexpressed in *E. coli*, and isolated by nickel chelate affinity chromatography (Fig. 7A). Marker rescue assays and constructed Ac*M*NPV recombinants demonstrated that P35-His_6 suppressed virus-induced apoptosis (data not shown). In in vitro assays using the tetrapeptide DEVD-amc as substrate, *Sf* protease activity was inhibited by wild-type P35-His_6 in a dose-dependent manner (Fig. 7B). Inhibition by functional P_3'(H90A-D91A)-mutated P35-His_6 paralleled that of wild-type P35-His_6. In contrast, loss-of-function P_1(D87A)-mutated P35-His_6 failed to inhibit *Sf* protease activity. Likewise, the protease inhibitory activity of P_4(D84A)-mutated P35-His_6 was diminished ~10,000-fold compared with wild-type P35-His_6 (Fig. 7B). P_1(D87A)- and P_4(D84A)-mutated P35-His_6 exhibited IC_{50}s of greater than 1,000 nM, whereas the IC_{50} of wild-type P35-His_6 was 70 pM (Table 2). Thus, the inability of P_1- and P_4-mutated P35 to inhibit *Sf* protease activity correlated with loss of P35 antiapoptotic activity.

P35-His_6 was also a potent in vitro inhibitor of tetrapeptide cleavage by recombinant hCPP32 and mICE, exhibiting IC_{50}s of 26 pM and 1.14 nM, respectively (Table 2). The capacity of P35-His_6 to inhibit 50% of the activity of hCPP32 and mICE at concentrations about half that of each protease indicated that a near-equimolar ratio of P35 to protease was sufficient for complete inhibition, confirming previous studies (3). As expected, P_1(D87A)-mutated P35-His_6 failed to inhibit hCPP32 and mICE (Table 2). However, in contrast to *Sf* protease activity, P_4(D84A)-mutated P35-His_6 was as effective in inhibiting hCPP32 and mICE (80 pM and 1.4 nM IC_{50}s, respectively) as was wild-type P35-His_6. Thus, the inhibition of hCPP32 and mICE by P_4(D87A)-mutated P35 distinguishes these vertebrate proteases from the baculovirus-induced *Sf* CED-3/ICE-like protease.

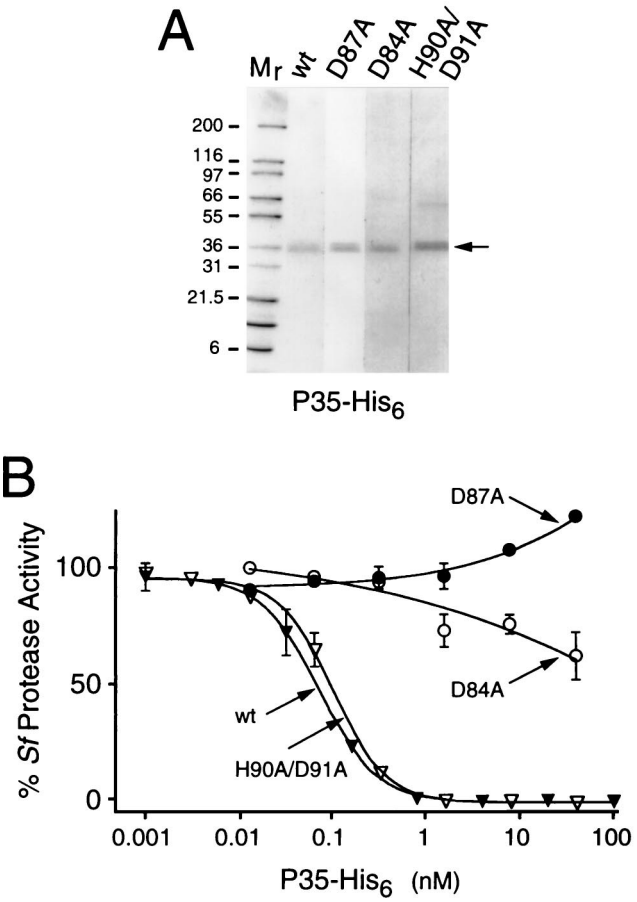

FIG. 7. P35-His_6 inhibition of virus-induced *Sf* CED-3/ICE-like protease. (A) Recombinant P35-His_6. After Ni^{2+} chelate chromatographic purification, wild-type (wt) and D87A-, D84A-, and H90A-D91A-mutated P35-His_6 were subjected to 14% polyacrylamide gel electrophoresis and stained with Coomassie brilliant blue. Molecular weight markers (M_r) are indicated. (B) P35-His_6 inhibition of *Sf* protease activity. Apoptotic extracts of vΔ35K-infected SF21 cells were preincubated with the indicated concentrations of wild-type (wt, closed triangles) and D87A-, D84A-, and H90A-D91A-mutated P35-His_6 and then assayed for protease activity using the tetrapeptide substrate DEVD-amc. Values are averages (± standard deviation) of duplicate determinations conducted in parallel and are expressed as a percentage of total protease activity. A single representative experiment is shown.

DISCUSSION

To investigate the mechanism by which P35 suppresses programmed cell death, we have identified protein domains required for P35 antiapoptotic activity in virus-infected cells, the function for which this baculovirus-encoded protein evolved. Since P35 prevents apoptosis induced by multiple signals in diverse organisms, it was expected that it targets a highly conserved step in the death pathway. We report here that P35 interacts with a novel CED-3/ICE-like protease (*Sf* protease) induced during baculovirus infection of *S. frugiperda* cells. As a consequence of this interaction, P35 is cleaved at or near the sequence DQMD-87G and inhibits the host protease activity. The P35 cleavage site substitution D87A eliminated in vivo and in vitro cleavage of P35, abolished P35-His_6 inhibition of the *Sf* protease, and caused loss of antiapoptotic activity. Thus, P35 interaction with and cleavage by the virus-induced CED-3/ICE-like *Sf* protease are required for suppression of virus-induced apoptosis. Collectively, our findings confirmed the CED-3/ICE protease inhibitory properties of P35 (3, 46) and support the hypothesis that P35 prevents programmed cell death in diverse organisms by inhibiting the CED-3/ICE-related proteases (Fig. 8). The effectiveness of P35 as a general apoptotic suppressor is therefore indicative of the critical role these proteases have in the cell death program.

TABLE 2. P35-His_6 IC_{50}s for inhibition of *Sf* protease, recombinant hCPP32, and mICE[a]

Protease	Substrate	P35-His_6 IC_{50} (nM)			
		WT	D87A	D84A	H90A-D91A
Sf protease	DEVD-amc	0.07	>1,000	>1,000	0.10
hCPP32	DEVD-amc	0.03	>1,000	0.08	0.04
mICE	YVAD-amc	1.14	>1,000	1.56	1.40

[a] Apoptotic extracts of vΔ35K-infected cells containing *Sf* protease or *E. coli* lysates containing recombinant hCPP32 (40 pM) or mICE (1.2 nM) were preincubated with increasing concentrations of wild-type (WT) or D87A-, D84A-, or H90A-D91A-mutated P35-His_6. Protease activity was measured by using tetrapeptide substrate DEVD-amc or YVAD-amc. Values are the averages of duplicate (*Sf* protease) or triplicate (hCPP32 and mICE) determinations conducted in parallel and are expressed as the P35-His_6 concentration required for 50% inhibition of protease activity. The ranges and standard deviations were less than 10% of the measured values.

Viral induction of a CED-3/ICE-like protease. Although full-length P35 was synthesized early in infection, P35 cleavage was not detected until apoptotic signs (blebbing and DNA fragmentation) appeared later in cells infected with *p35* null mutants (Fig. 3B). This finding was consistent with P35 interaction with the CED-3/ICE-like *Sf* protease that is activated after the initiation of virus infection. Indeed, *Sf* protease activity was detected only in SF21 cells induced to undergo apoptosis by virus infection or actinomycin D treatment (Fig. 6 and data not shown). As expected for a CED-3/ICE-related protease, the *Sf* protease cleaved P35 in an Asp-87-dependent manner (Fig. 4 and 5) that was blocked by ICE-specific inhibitors (Fig. 6). Selective inhibition by the tetrapeptide DEVD-CHO, but not YVAD-CHO (Fig. 6), suggested that substrate specificity of the *Sf* protease more closely resembles that of CPP32 and MCH3 than that of ICE (11, 29). Nonetheless, the virus-induced *Sf* protease was distinct from the recombinant mammalian proteases on the basis of its resistance to inhibition by D84A-substituted P35-His_6 (Table 2). The identification of a baculovirus-induced CED-3/ICE-like protease activity in insect cells, combined with the finding that P35 is a potent inhibitor of this *Sf* protease activity, supports the conclusion that host cell apoptosis is due to viral induction of a death protease. As such, our data provide direct evidence that an animal virus can directly or indirectly activate a CED-3/ICE-like protease that is subsequently inhibited by direct interaction with a virus-encoded protein. The apoptotic signals induced by infection must therefore lie upstream from the step involving these proteases in the death pathway (Fig. 8). The molecular nature of the baculovirus-specific signals remains to be determined.

Mechanism of P35 interaction and inhibition of CED-3/ICE-like proteases. Our study and those of others (3, 46) indicate that P35 is both a substrate and an inhibitor of CED-3/ICE family proteases. Complete protease inhibition was achieved by a near-equimolar ratio of purified P35 to hCPP32, mICE, hICE, ICH-1, and ICH-2 (Table 2) (3). The direct correlation between P35 cleavage, protease inhibition, and antiapoptotic function as demonstrated here is consistent with a model wherein CED-3/ICE protease inhibition is mediated by P35 cleavage products (3). The observation that P35 cleavage products are capable of forming stable complexes with human ICE (3) raises the possibility that P35 inhibition involves a cleavage product-inhibited enzyme complex analogous to that formed during protease inhibition by the serpins (reviewed in reference 31). Nonetheless, P35 bears no sequence similarity to any known serpin.

As expected for proteases with Asp-X peptide bond specificity (41), cleavage of P35 by the *Sf* protease, hCPP32, mICE, and CED-3 was abolished by Ala substitution of the P_1 Asp residue (D87A) (Fig. 4 and 5) (46). The D87A substitution also abolished the protease inhibitory activity of recombinant P35-His_6 (Fig. 7). Thus, the P_1 Asp residue affects protease binding, P35 cleavage, or both. Neither our data nor those of previous studies distinguish these possibilities. Several substitutions N terminal to the scissile bond also caused P35 loss of in vivo and in vitro function (Fig. 4 and 7). In particular, D84A substitution of the P_4 Asp residue caused loss of P35 antiapoptotic activity and reduced *Sf* protease inhibitory activity of P35-His_6 more than 10,000-fold (Fig. 4; Table 2). However, unlike P_1-substituted P35, cleavage of P_4-substituted P35 by the *Sf* protease was readily detected in vivo and in vitro (Fig. 4 and 5). This finding raises the possibility that the P_4 residue affects postcleavage events required for protease inhibition, including, for example, retention of the P35 cleavage products by the protease complex. As such, P_4 substitutions could convert P35 from a substrate inhibitor to a substrate alone by allowing cleavage product dissociation. Alternatively, since the P_4 residue affects the substrate specificity of ICE (41), Asp-84 may influence P35 binding to the *Sf* protease. Thus, despite the detection of P35 cleavage, P_4 substitutions may reduce P35-protease binding below that required for complete protease inhibition and subsequent suppression of apoptosis. A rigorous kinetic analysis of P35-protease interaction is required to distinguish the possible mechanistic differences between loss-of-function mutations of P_1 and P_4.

Multiple domains are required for P35 function. Besides mutations at or near the CED-3/ICE-like cleavage site, we identified other loss-of-function mutations, including several at the N and C termini of P35 (Fig. 1). These mutations may define residues required for pre- or postcleavage association of P35 with its target protease. Alternatively, they may define other protein interactions critical to P35 function or P35 stability. Of the *p35* mutations tested, all loss-of-function mutations caused reduced P35 accumulation in apoptotic cells (Fig. 2C). Although this reduction was due in part to decreased protein synthesis in apoptotic cells, our data indicated that P35 stability is unusually sensitive to mutagenesis. Only loss-of-function mutations in83 and ca79, located within or near a predicted α-helix (residues 62 to 80) adjacent to the CED-3/ICE-like cleavage site, had no effect on P35 accumulation, as indicated by normal P35 levels in apoptosis-resistant TN368 cells (Fig. 2C). This domain apparently has little effect on P35 stability and may be functionally analogous to the reactive site loop of the serpins (23, 31).

In contrast, charged-to-alanine mutations within CHR1 (ca17 and ca26) destabilized P35 in both apoptotic and nonapoptotic cells (Fig. 2C). Both mutations are located within

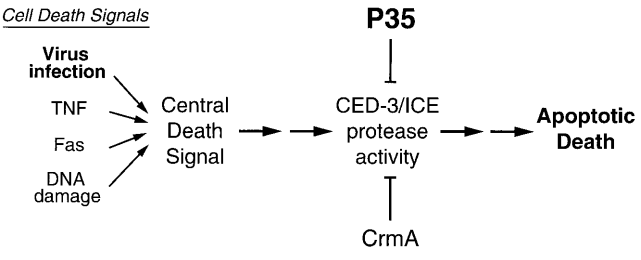

FIG. 8. Model for virus induction of the programmed cell death pathway. Diverse signals, including virus infection, tumor necrosis factor (TNF), Fas, or DNA damage, lead to the induction of a centralized cell death signal that in turn causes activation of the CED-3/ICE-related death proteases. Baculovirus P35 or cowpox virus CrmA prevent apoptotic death at a common step by inhibiting either proenzyme activation or the activity of CED-3/ICE-related cysteine proteases.

N-terminal sequences of $p35^{1-76}$ which upon constitutive expression in stably transfected cells dominantly interfere with antiapoptotic activity of wild-type *p35* (4). Since $p35^{1-76}$ may constitute a domain(s) that mediates interaction with P35 itself or other proteins required for P35 function, the CHR1 mutations may disrupt such protein interactions. The oligomeric state of P35 required for efficient CED-3/ICE protease inhibition and P35 stability is under investigation.

ACKNOWLEDGMENTS

We thank Gulam Manji and Pam Hershberger in particular for construction of plasmids and viruses used in this study. We also acknowledge Kim Hoang for technical assistance and Lawrence Fritz for helpful discussions.

This work was supported in part by Public Health Service grant AI25557 from the National Institute of Allergy and Infectious Diseases (P.D.F.) and a Markey Foundation grant to the Institute for Molecular Virology.

REFERENCES

1. **Beidler, D. R., M. Tewari, P. D. Friesen, G. Poirier, and V. M. Dixit.** 1995. The baculovirus p35 protein inhibits Fas- and tumor necrosis factor-induced apoptosis. J. Biol. Chem. **270:**16526–16528.
2. **Boulakia, C. A., G. Chen, F. W. H. Ng, J. G. Teodoro, P. E. Branton, D. W. Nicholson, G. G. Poirer, and G. C. Shore.** 1996. Bcl-2 and adenovirus E1B 19 kDa protein prevent E1A-induced processing of CPP32 and cleavage of poly(ADP-ribose) polymerase. Oncogene **12:**529–535.
3. **Bump, N. J., M. Hackett, M. Hugunin, S. Seshagriri, K. Brady, P. Chen, C. Ferenz, S. Franklin, T. Ghayur, L. P., P. Licari, J. Mankovich, L. Shi, A. H. Greenberg, L. K. Miller, and W. W. Wong.** 1995. Inhibition of the ICE family proteases by baculovirus antiapoptotic protein p35. Science **269:**1885–1888.
4. **Cartier, J. L., P. A. Hershberger, and P. D. Friesen.** 1994. Suppression of apoptosis in insect cells stably transfected with baculovirus *p35*: dominant interference by N-terminal sequences $p35^{1-76}$. J. Virol. **68:**7728–7737.
5. **Chiou, S. K., L. Rao, and E. White.** 1994. Bcl-2 blocks p53-dependent apoptosis. Mol. Cell. Biol. **14:**2556–2563. (Erratum, **14:**4333.)
6. **Clem, R. J., M. Fechheimer, and L. K. Miller.** 1991. Prevention of apoptosis by a baculovirus gene during infection of insect cells. Science **254:**1388–1390.
7. **Clem, R. J., and L. K. Miller.** 1993. Apoptosis reduces both the in vitro replication and the in vivo infectivity of a baculovirus. J. Virol. **67:**3730–3738.
8. **Clem, R. J., and L. K. Miller.** 1994. Control of programmed cell death by the baculovirus genes *p35* and *iap*. Mol. Cell. Biol. **14:**5212–5222.
9. **Crook, N. E., R. J. Clem, and L. K. Miller.** 1993. An apoptosis-inhibiting baculovirus gene with a zinc finger-like motif. J. Virol. **67:**2168–2174.
10. **Fernandes-Alnemri, T., G. Litwack, and E. S. Alnemri.** 1994. CPP32, a novel human apoptotic protein with homology to Caenorhabditis elegans cell death protein Ced-3 and mammalian interleukin-1 beta-converting enzyme. J. Biol. Chem. **269:**30761–30764.
11. **Fernandes-Alnemri, T., A. Takahashi, R. Armstrong, J. Krebs, L. Fritz, K. J. Tomaselli, L. Wang, Z. Yu, C. M. Croce, G. Salveson, W. C. Earnshaw, G. Litwack, and E. S. Alnemri.** 1995. Mch3, a novel human apoptotic cysteine protease highly related to CPP32. Cancer Res. **55:**6045–6052.
12. **Gregory, C. D., C. Dive, S. Henderson, C. A. Smith, G. T. Williams, J. Gordon, and A. B. Rickinson.** 1991. Activation of Epstein-Barr virus latent genes protects human B cells from death by apoptosis. Nature (London) **349:**612–614.
13. **Grether, M. E., J. M. Abrams, J. Agapite, K. White, and H. Steller.** 1995. The *head involution defective* gene of *Drosophila melanogaster* functions in programmed cell death. Genes Dev. **9:**1694–1708.
14. **Hay, B. A., T. Wolff, and G. M. Rubin.** 1994. Expression of baculovirus P35 prevents cell death in *Drosophila*. Development (Cambridge) **120:**2121–2129.
15. **Henderson, S., D. Huen, M. Rowe, C. Dawson, G. Johnson, and A. Rickinson.** 1993. Epstein-Barr virus-encoded BHRF1 protein, a viral homologue of Bcl-2, protects human B cells from programmed cell death. Proc. Natl. Acad. Sci. USA **90:**8479–8483.
16. **Hengartner, M. O., and H. R. Horvitz.** 1994. Programmed cell death in Caenorhabditis elegans. Curr. Opin. Genet. Dev. **4:**581–586.
17. **Hershberger, P. A., J. A. Dickson, and P. D. Friesen.** 1992. Site-specific mutagenesis of the 35-kilodalton protein gene encoded by *Autographa californica* nuclear polyhedrosis virus: cell line-specific effects on virus replication. J. Virol. **66:**5525–5533.
18. **Hershberger, P. A., D. J. LaCount, and P. D. Friesen.** 1994. The apoptotic suppressor P35 is required early during baculovirus replication and is targeted to the cytosol of infected cells. J. Virol. **68:**3467–3477.
19. **Hink, W. F.** 1970. Established insect cell line from cabbage looper, *Trichoplusia ni*. Nature (London) **225:**466–467.
20. **Kamita, S. G., K. Majima, and S. Maeda.** 1993. Identification and characterization of the p35 gene of *Bombyx mori* nuclear polyhedrosis virus that prevents virus-induced apoptosis. J. Virol. **67:**455–463.
21. **Kunkel, T. A., J. D. Roberts, and R. A. Zakour.** 1987. Rapid and efficient site-specific mutagenesis without phenotypic selection. Methods Enzymol. **154:**367–382.
22. **Korsmeyer, S. J.** 1995. Regulators of cell death. Trends Genet. **11:**101–105.

22a. **LaCount, D.** Unpublished data.

23. **Lawrence, D. A., D. Ginsburg, D. E. Day, M. B. Berkenpas, I. M. Verhamme, J. Kvassman, and J. D. Shore.** 1995. Serpin-protease complexes are trapped as stable acyl-enzyme intermediates. J. Biol. Chem. **270:**25309–25312.
24. **Lazebnik, Y. A., S. H. Kaufmann, S. Desnoyers, G. G. Poirier, and W. C. Earnshaw.** 1994. Cleavage of poly(ADP-ribose) polymerase by a proteinase with properties like ICE. Nature (London) **371:**346–347.
25. **Levine, B., Q. Huang, J. T. Isaacs, J. C. Reed, D. E. Griffin, and J. M. Hardwick.** 1993. Conversion of lytic to persistent alphavirus infection by the bcl-2 cellular oncogene. Nature (London) **361:**739–742.
26. **Martin, S. J., and D. R. Green.** 1995. Protease activation during apoptosis: death by a thousand cuts? Cell **82:**349–352.
27. **Martinou, I., P. A. Fernandez, M. Missotten, E. White, B. Allet, R. Sadoul, and J. C. Martinou.** 1995. Viral proteins E1B 19K and p35 protect sympathetic neurons from cell death induced by NGF deprivation. J. Cell Biol. **128:**201–208.
28. **Neilan, J. G., Z. Lu, C. L. Afonso, G. F. Kutish, M. D. Sussman, and D. L. Rock.** 1993. An African swine fever virus gene with similarity to the proto-oncogene *bcl-2* and the Epstein-Barr virus gene *BHRF1*. J. Virol. **67:**4391–4394.
29. **Nicholson, D. W., A. Ali, N. A. Thornberry, J. P. Vaillancourt, C. K. Ding, M. Gallant, Y. Gareau, P. R. Griffin, M. Labelle, Y. A. Lazebnik, N. A. Munday, S. M. Raju, M. E. Smulson, T. Yamin, V. Yu, and D. K. Miller.** 1995. Identification and inhibition of the ICE/CED-3 protease necessary for mammalian apoptosis. Nature (London) **376:**37–43.
30. **Pocker, Y., and J. T. Stone.** 1967. The catalytic versatility of erythrocyte carbonic anhydrase III. Kinetic studies of the enzyme-catalyzed hydrolysis of p-nitrophenyl acetate. Biochemistry **6:**668–678.
31. **Potempa, J., E. Korzus, and J. Travis.** 1994. The serpin superfamily of proteinase inhibitors: structure, function, and regulation. J. Biol. Chem. **269:**15957–15960.
32. **Rabizadeh, S., D. J. LaCount, P. D. Friesen, and D. E. Bredesen.** 1993. Expression of the baculovirus p35 gene inhibits mammalian neural cell death. J. Neurochem. **61:**2318–2321.
33. **Rao, L., M. Debbas, P. Sabbatini, D. Hockenbery, S. Korsmeyer, and E. White.** 1992. The adenovirus E1A proteins induce apoptosis, which is inhibited by the E1B 19-kDa and Bcl-2 proteins. Proc. Natl. Acad. Sci. USA **89:**7742–7746.
34. **Ray, C. A., R. A. Black, S. R. Kronheim, T. A. Greenstreet, P. R. Sleath, G. S. Salvesen, and D. J. Pickup.** 1992. Viral inhibition of inflammation: cowpox virus encodes an inhibitor of the interleukin-1β converting enzyme. Cell **69:**597–604.
35. **Shen, Y., and T. E. Shenk.** 1995. Viruses and apoptosis. Curr. Opin. Genet. Dev. **5:**105–111.
36. **Steller, H.** 1995. Mechanisms and genes of cellular suicide. Science **267:** 1445–1449.
37. **Sugimoto, A., P. D. Friesen, and J. H. Rothman.** 1994. Baculovirus p35 prevents developmentally programmed cell death and rescues a ced-9 mutant in the nematode *Caenorhabditis elegans*. EMBO J. **13:**2023–2028.
38. **Tewari, M., and V. M. Dixit.** 1995. Fas- and tumor necrosis factor-induced apoptosis is inhibited by the poxvirus crmA gene product. J. Biol. Chem. **270:**3255–3260.
39. **Tewari, M., L. Quan, K. O'Rourke, S. Desnoyers, Z. Zeng, D. R. Beidler, G. G. Poirier, G. S. Salvesen, and V. M. Dixit.** 1995. Yama/CPP32 beta, a mammalian homolog of CED-3, is a CrmA-inhibitable protease that cleaves the death substrate poly(ADP-ribose) polymerase. Cell **81:**801–809.
40. **Thompson, C. B.** 1995. Apoptosis in the pathogenesis and treatment of disease. Science **267:**1456–1462.
41. **Thornberry, N. A., and S. M. Molineaux.** 1995. Interleukin-1β converting enzyme: a novel cysteine protease required for IL-1β production and implicated in programmed cell death. Protein Sci. **4:**3–12.
42. **Vaughn, J. L., R. H. Goodwin, G. J. Tompkins, and P. McCawley.** 1977. The establishment of two cell lines from the insect Spodoptera frugiperda (Lepidoptera; Noctuidae). In Vitro (Rockville) **13:**213–7.
43. **Vaux, D. L., G. Haecker, and A. Strasser.** 1994. An evolutionary perspective on apoptosis. Cell **76:**777–779.
44. **Wang, L., M. Miura, L. Bergeron, H. Zhu, and J. Yuan.** 1994. Ich-1, an *Ice/ced-3*-related gene, encodes both positive and negative regulators of programmed cell death. Cell **78:**739–750.
45. **White, E.** 1996. Life, death, and the pursuit of apoptosis. Genes Dev. **10:**1–15.
46. **Xue, D., and H. R. Horvitz.** 1995. Inhibition of the *Caenorhabditis elegans* cell-death protease CED-3 by a CED-3 cleavage site in baculovirus p35 protein. Nature (London) **377:**248–251.
47. **Yuan, J., S. Shaham, S. Ledoux, H. M. Ellis, and H. R. Horvitz.** 1993. The *C. elegans* cell death gene *ced-3* encodes a protein similar to mammalian interleukin-1 beta-converting enzyme. Cell **75:**641–652.